Boosting the lithium transport in phase-change polymer electrolytes towards stable cycling lithium metal batteries with thermal-robustness

Yulong He[1], *Zicheng Luo*[1], *Hongfei Xu*[1], *Zehong Yuan*[1,2], *Songmei Li*[1], *Shubin Yang*[1]*, *Bin Li*[1,2]*

1. School of Materials Science & Engineering, Beihang University, Beijing, 100191, China

2. National Experimental Teaching Demonstration Center for Materials Science and Engineering (Beihang University), Beijing, 100191, China

*E-mail: li_bin@buaa.edu.cn, yangshubin@buaa.edu.cn

Experimental Section

Materials

Polycaprolactone (PCL, Mn=65000, hydroxyl terminating), dimethyl dodecanedioate (DDCA), bis(trifluoromethane)sulfonimide lithium salt (LiTFSI), and propylene carbonate (PC) were all purchased from Innochem. The PCL-DDCA electrolyte is prepared by simply blending raw materials to form a uniform phase. Specifically, 0.5 g PCL and 0.5 g DDCA were added into a vital and then were heated at 70 ℃ to make them melt completely. It should be noted the preheating of DDCA is necessary because the melting point of DDCA is ~33 ℃. Then 0.3 g LiTFSI was added into above clear solution under vigorous stirring until completely dissolved, obtaining the PCL-DDCA electrolyte. To further improve the ionic conductivity of PCL-DDCA electrolyte, using PC (0.25 g) as plasticizer to replace the 50 wt% of DDCA, and the mixtures were stirred by magnetic agitation and heated at 70 °C overnight. The resultant viscous/clear PCL-DDCA-PC electrolyte was obtained. Other control group was prepared via the same method as PCL-DDCA-PC electrolyte. For instance, DDCA-PC-LiTFSI was obtained except without PCL, PCL-LiTFSI was obtained except without DDCA and PC. All these preparations were conducted in an Ar glove box with low-level water and oxygen content**.**

Characterization

XRD patterns were recorded using a D8 discover X-ray diffractometer with Cu Kα radiation. Fourier transform infrared spectrometer (FT-IR) (Thermo Nicolet Corporation; 4000-400/cm 0.09/cm/6700) was used to analyze the samples. The morphology of the as-prepared PCL-DDCA-PC electrolyte was observed by scanning electron microscopy (SEM, SU8020). Differential scanning calorimetry (STA-449F5) was carried out to characterize the heat-storage capacity and specific heat of samples in the range from -20 °C to 60 °C at a heating rate of 10 °C min^{-1}. The thermographic images of the pouch cell (40 mm × 60 mm) heated on the hot plate (60 °C)/ frozen on the cold plate (5 °C) were photographed by an infrared imager.

Electrochemical measurements

The stainless steel (SS)/ PCL-DDCA-PC electrolyte /SS cells were assembled EIS was assembled to measure the ionic conductivity with a frequency range from 0.1 Hz to 100 kHz. The electrochemical impedance spectroscopy (EIS) was measured in the temperature range from 20 °C to 60 °C (record every 5 °C). The ionic conductivity was calculated by the following equation:

$$\sigma = \frac{L}{R_b S} \qquad (1)$$

where σ, L, R_b, S represent the ionic conductivity, thickness, bulk resistance of PCL-DDCA-PC electrolyte, respectively. And S represents the contact area between the two stainless steel plates. Considering that since PCL-DDCA-PC electrolyte does not have self-supporting properties, we use a hollow ring gasket made of polytetrafluoroethylene to support PCL-DDCA-PC electrolyte. As the thickness and hollow area of the gasket are determined, the thickness of the PCL-DDCA-PC electrolyte and its contact area with the electrode are also constant, 0.509 mm and 1.1304 cm^{-2}, respectively.

The activation energy (E_a) was calculated according to the Arrhenius law:

$$\sigma = \sigma_0 exp\left(-\frac{E_a}{kT}\right)$$

$$lg\sigma = lg\sigma_0 - \frac{lgeE_a}{kT}$$

Where σ_0 is the finger-forward factor (S cm^{-1}), E_a is the ion mobility activation energy (eV), K is the Boltzmann's constant, and T is the Kelvin temperature (K).

Li^+ Transference Number can be tested using Li/ PCL-DDCA-PC electrolyte electrolyte /Li symmetric cells at 30 °C. The cell resistances are determined before and after polarization using EIS and currents measured by the DC method. t_{Li+} is obtained according to the following Equation (3):

$$t_{Li+} = \frac{I_s(\Delta V - I_0 R_0)}{I_0(\Delta V - I_s R_s)} \qquad (3)$$

Where I_0 and I_s are the initial and steady-state currents. The R_0 and R_s are the resistances before and after polarization of the cell, respectively. Δ V is the DC potential applied across the cell.

LSV was conducted from 1.5 to 6 V with the scan rate of 1 mV s^{-1} to test the electrochemical window of Li/PCL-DDCA-PC electrolyte/SS cells. CV was tested at a scan rate of 0.5 mV s^{-1} for $LiFePO_4$. All the above measurements were conducted using a CHI 660D electrochemical workstation (Chenhua Instruments Co., China).

The $LiFeO_4$ (LFP) and $LiNi_{0.8}Co_{0.1}Mn_{0.1}O_2$ (NCM) cathode materials are obtained from Canrd Technology Co., Ltd. The cathode slurry was prepared by mixing LFP/NCM powder, Super P, and polyvinylidene fluoride binder at a weight ratio of 8:1:1 in N-methyl-2-pyrrolidone (NMP) solvent and magnetically stirred overnight. Then coated on Al foil with an active material mass loading of 1.5-2 mg cm^{-2} and dried

at 60 °C for 12 h to remove the NMP in a vacuum oven. The cathode layer was cut into disks of 12 mm diameter. CT2001A battery testing system (Wuhan LAND Electronic Co., Ltd, China) at 30 °C. The charge and discharge tests of Li|LFP and Li|NCM full cells were carried out at 2.5-3.8 V (1 C = 170 mA g^{-1}) and 2.8-4.2 V (1 C = 188 mA g^{-1}), respectively.

Pouch cells (size: 40 mm × 60 mm) were assembled with high mass-loading (14 mg cm^{-2}) $LiFePO_4$, PCL-DDCA-PC electrolyte and Li belt, which was used for the thermal/cold shock resistance test. Notably, the glass fiber separator serves as supporter for PCL-DDCA-PC electrolyte when assembling pouch cell. For comparison, a common liquid electrolyte of same mass as PCL-DDCA-PC electrolyte was used to assemble $LiFePO_4$/liquid electrolyte/Li pouch cells. The commercial liquid electrolyte was composed of 1M lithium bistrifluoromethanesulfonimide (LiTFSI) with 0.1M $LiNO_3$ in 1,3-dioxolane (DOL) and 1,2-dimethoxyethane (DME) binary solvent (1:1 in volume).
The nail (ϕ = 5 mm) penetration test was conducted on $LiFePO_4$/ PCL-DDCA-PC electrolyte /Li pouch cells (size: 20 mm × 30 mm). Before nail penetration, the cells were galvanostatically charged to 100% state of charge. A nail was penetrated in the center of the fully charged cells.

MD Calculation details

The molecular dynamics (MD) calculations were conducted using BIOVIA Materials Studio (MS, Accelrys Software Inc. San Diego,USA). The COMPASS II force field was used. The electrostatic interaction was calculated using the Ewald summation method and the van der Waals interaction. The structure of Li^+, $TFSI^-$, CL, DDCA and PC molecular were drawn by the "visualizer" module. Due to calculation limitations, PCL chain segment containing 19 CL monomers (denoted as PCL2000) was used during the calculations to simulate the effect of PCL chains. PCL2000 was constructed via the "homopolymer" module. Relaxation, geometry and energy optimization and anneal were performed on these structures.
The original models of the PCL-DDCA-PC were generated by the "amorphous cell" module. The lattice type was set as cubic, and the input density of the cell was 0.97 g cm^{-3}. Each cell was composed of 10 Li^+ cations and 10 $TFSI^-$ anions, 3 PCL2000, 20 DDCA and 20 PC molecular. The output was 50 cells. After selecting the cells with the lowest energy, further optimization was carried out. The cells were relaxed using the "smart minimizer" method to minimize the system energy. Then, 100 ps MD simulations were performed successively in the NVT ensemble and the NPT ensemble at 303 K, accordingly, for the final optimization. The radial distribution function (RDF) can be acquired through an analysis of the optimized model.

Calculation details

To furtherly investigate the thermal robustness of the PCL-DDCA-PC electrolyte, a CFD cell package model is developed using the ANSYS Fluent software package. The

3D structure of the cell package is drawn on SpaceClaim. Each cell of the pack measures 90mm in length, 140mm in width, and 10mm in thickness. There are a total of five cells, designated as cell1, cell2, cell3, cell4, and cell5. Subsequently, the established model is subjected to grid division, with a minimum grid size of 0.2mm. After optimization, the next step is initiated. In ANSYS Fluent, firstly, within the General Settings, the time is configured as "transient." Then, in the "Model Settings," the "energy" option is activated, along with the "battery model." In the "Model Options," the "NGTK Empirical Model" is enabled, specifying the Nominal Cell Capacity as 30 Ah and designating the C-rate as 1. Following the setup of conductive zones and electric contacts, it is essential to activate the "thermal abuse model" within the "Advanced Options," selecting the "four-equation kinetics model." In the "Material Settings," the parameters for both PCL-DDCA-PC electrolyte and commercial liquid electrolyte, such as density, specific heat capacity, and thermal conductivity, are input to create the materials. After configuring the computational domain and boundary conditions, "flow" and 'turbulence' are deactivated within "Control." Initialization is carried out subsequently. Finally, a spherical short-circuit area with a radius of 5 mm is patched, with an electrical resistance set at 5e-8 ohms to simulate a short circuit within the battery pack. The calculation is then initiated.

DFT Computational methods

All computations were performed using the Gaussian 16 software package. The density functional M06-2X combined with the D3 dispersion correction was employed, and 6-31G(d,p) basis set was used for all atoms. Both structural optimization and frequency analysis were performed at this same level of theory. All optimized structures have satisfied the default convergence criteria and exhibit no imaginary frequencies. Electronic structures were obtained from single-point DFT calculations using the M06-2X functionals with the 6-311G(d,p) basis set. The interaction energy (ΔE_{int}) is calculated as the difference between the total energy of the complex and the sum of total energies of its components.

$$E_{int} = E_{total} - \sum E_{component}$$

where E_{total} presents the total energy of the system and $E_{component}$ presents the energy of each component. The higher absolute value of the $-E_{int}$ demonstrates a stronger interaction.

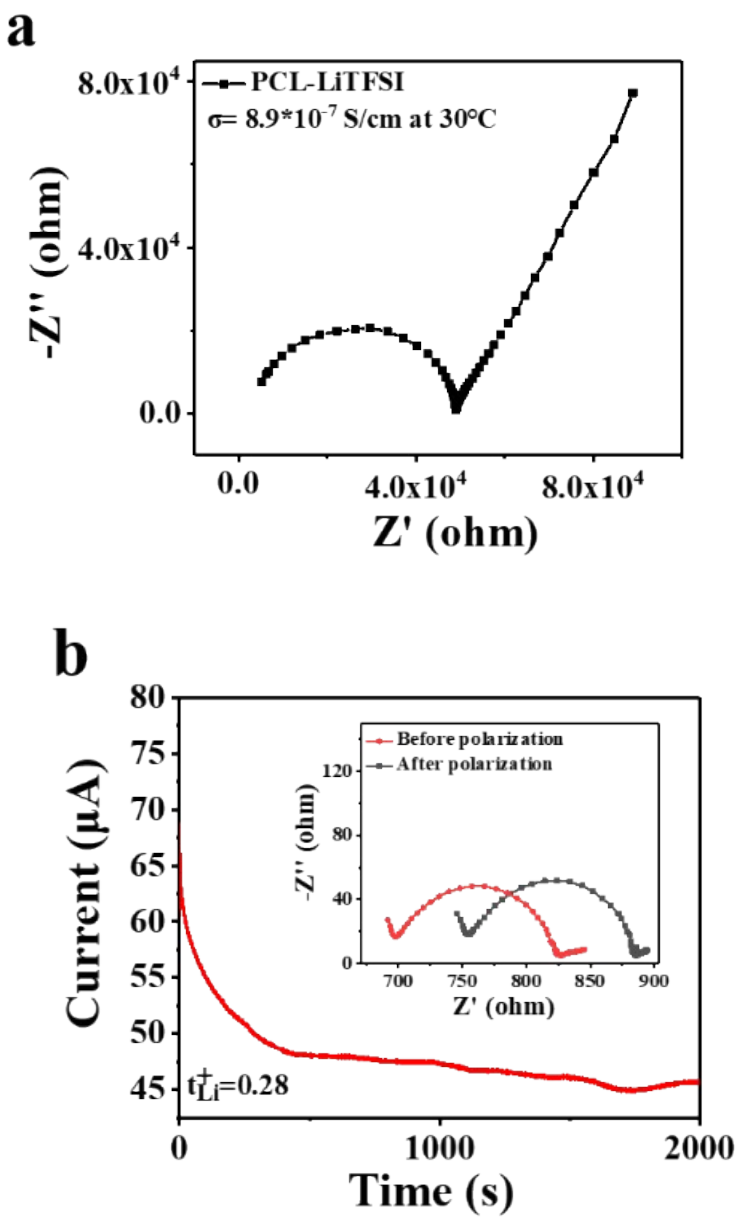

Fig. S1 (a) The EIS curve of PCL-LiTFSI electrolyte and (b) its lithium ion transfer number.

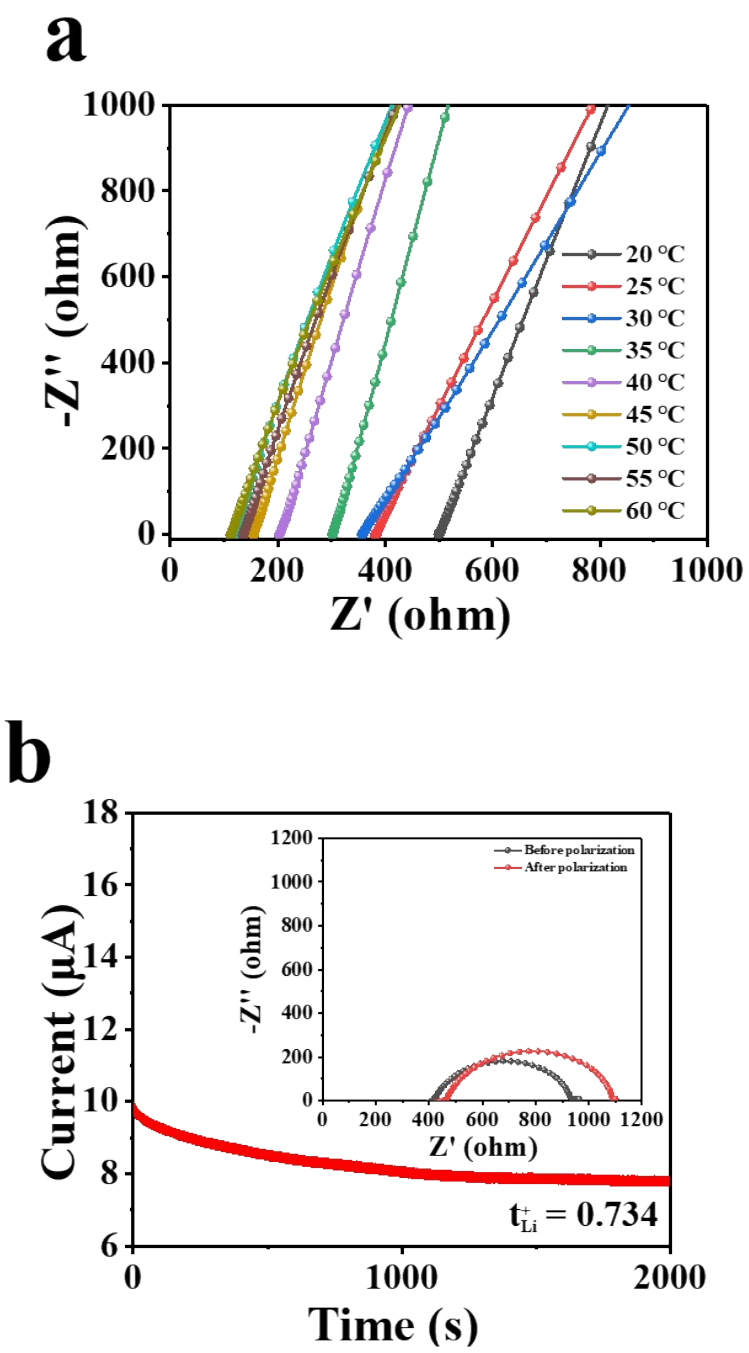

Fig. S2 (a) Arrhenius plots of the ionic conductivities of the PCL-DDCA electrolytes at 20–60°C and (b) its lithium ion transfer number.

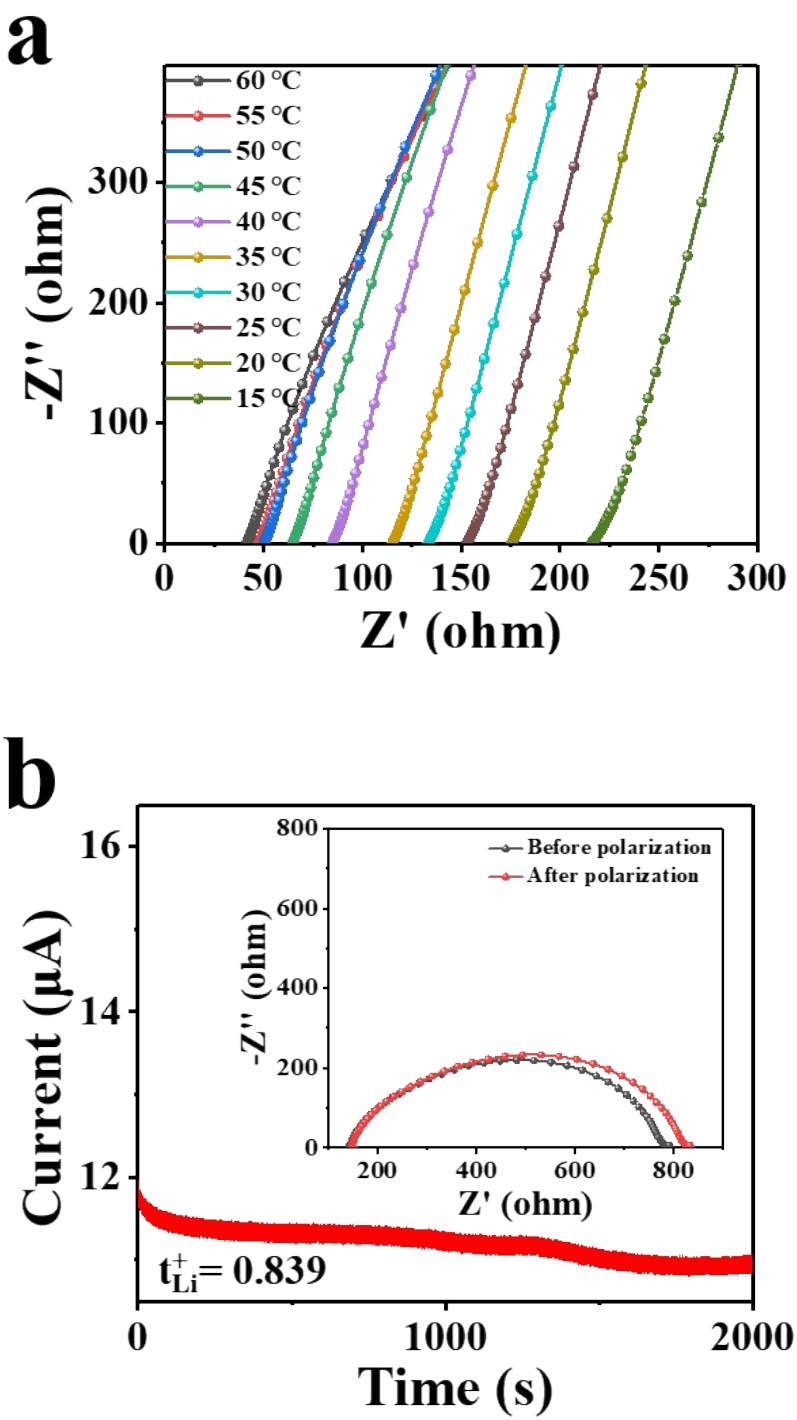

Fig. S3 (a) The EIS curves of the PCL-DDCA-PC electrolytes at 15–60°C and (b) its lithium ion transfer number.

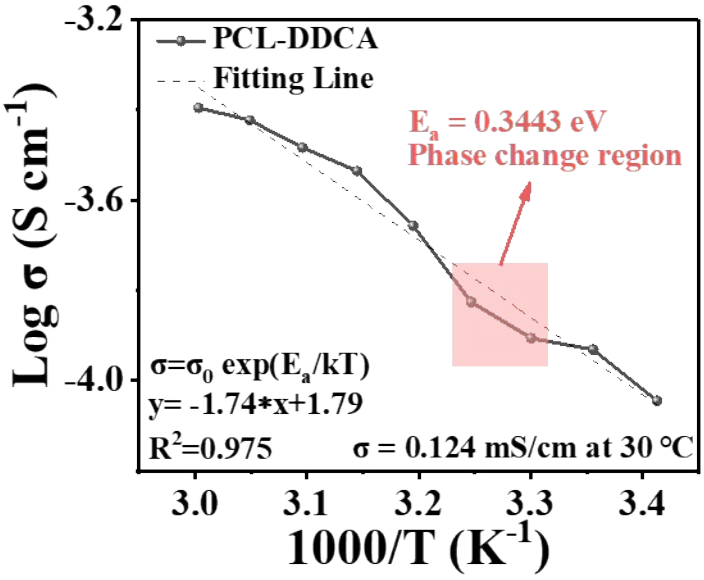

Fig. S4 Arrhenius plots illustrating the relationship between ionic conductivity and temperature for the PCL-DDCA electrolyte.

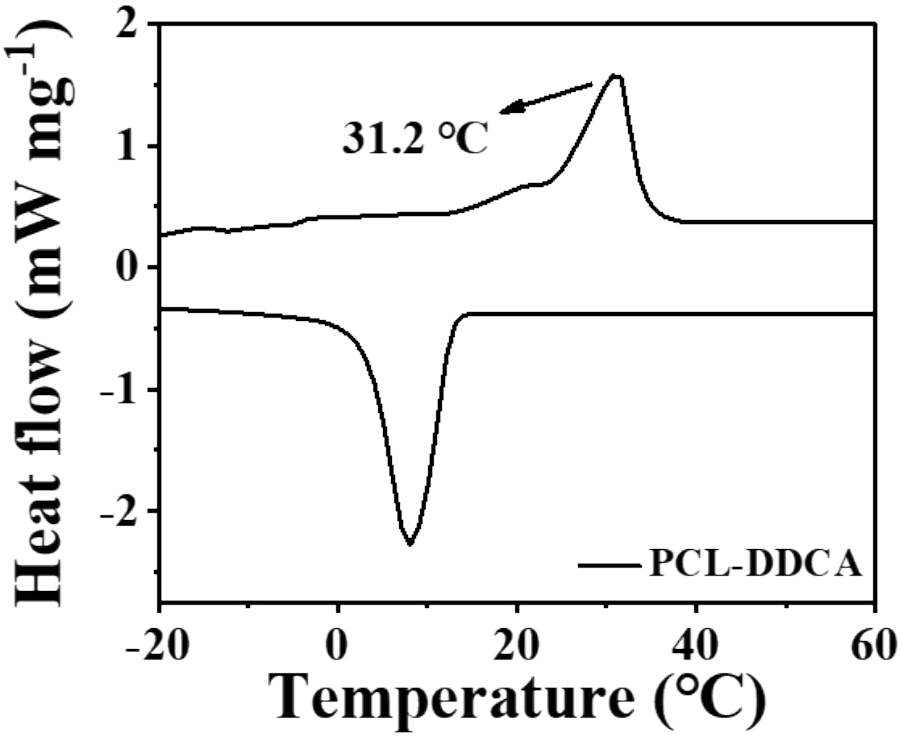

Fig. S5 DSC thermograms of PCL-DDCA- electrolyte.

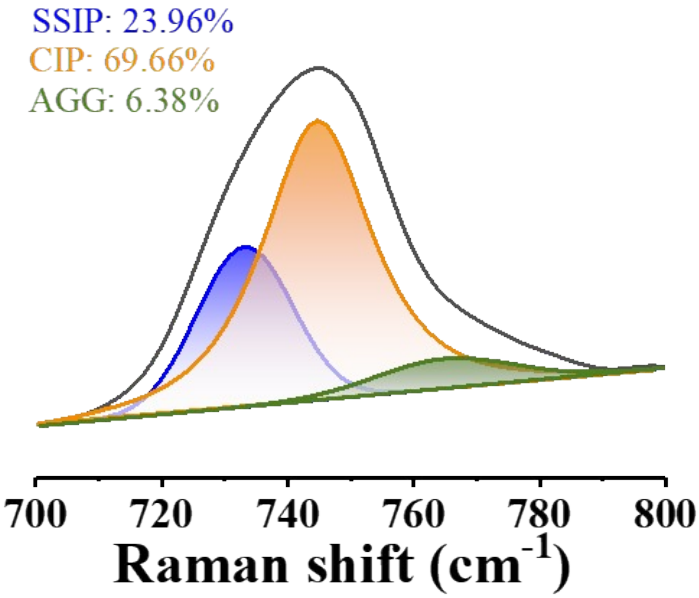

Fig. S6 Raman fitting results of TFSI- coordination in PCL-LiTFSI electrolyte.

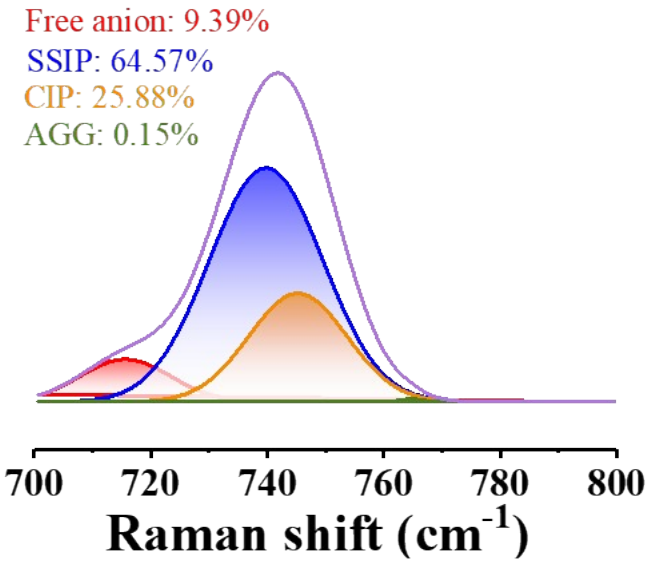

Fig. S7 Raman fitting results of TFSI- coordination in DDCA-PC-LiTFSI electrolyte.

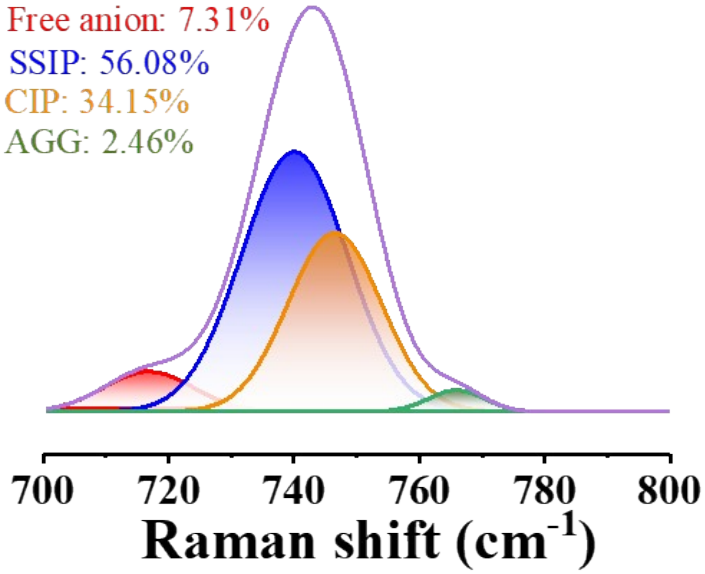

Fig. S8 Raman fitting results of TFSI- coordination in PCL-DDCA-PC-LiTFSI electrolyte.

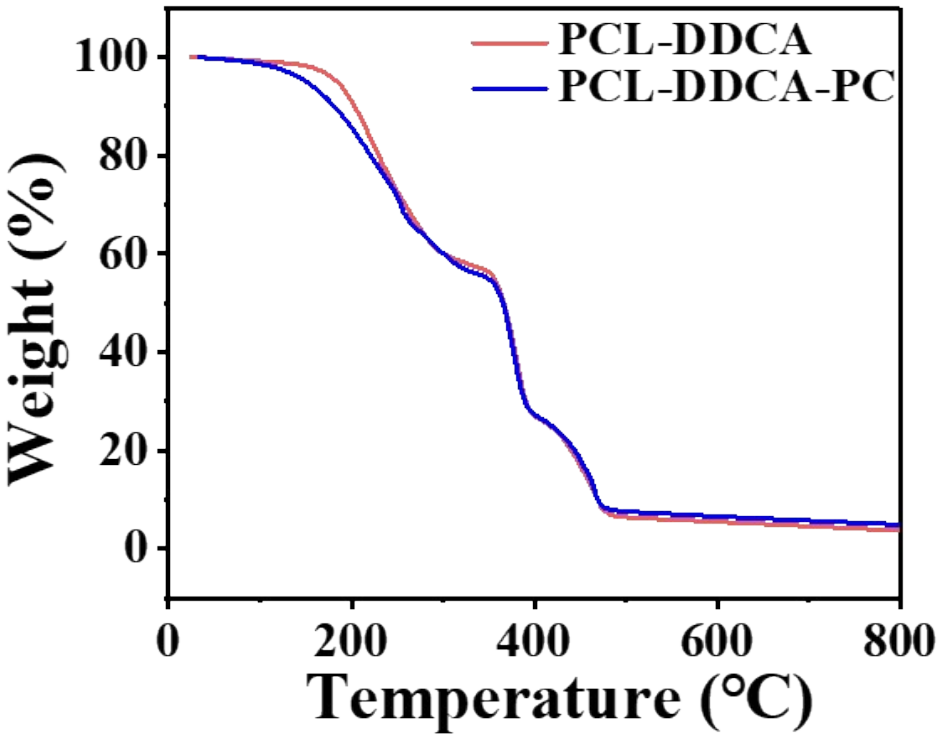

Fig. S9 The TGA curves of different electrolyte.

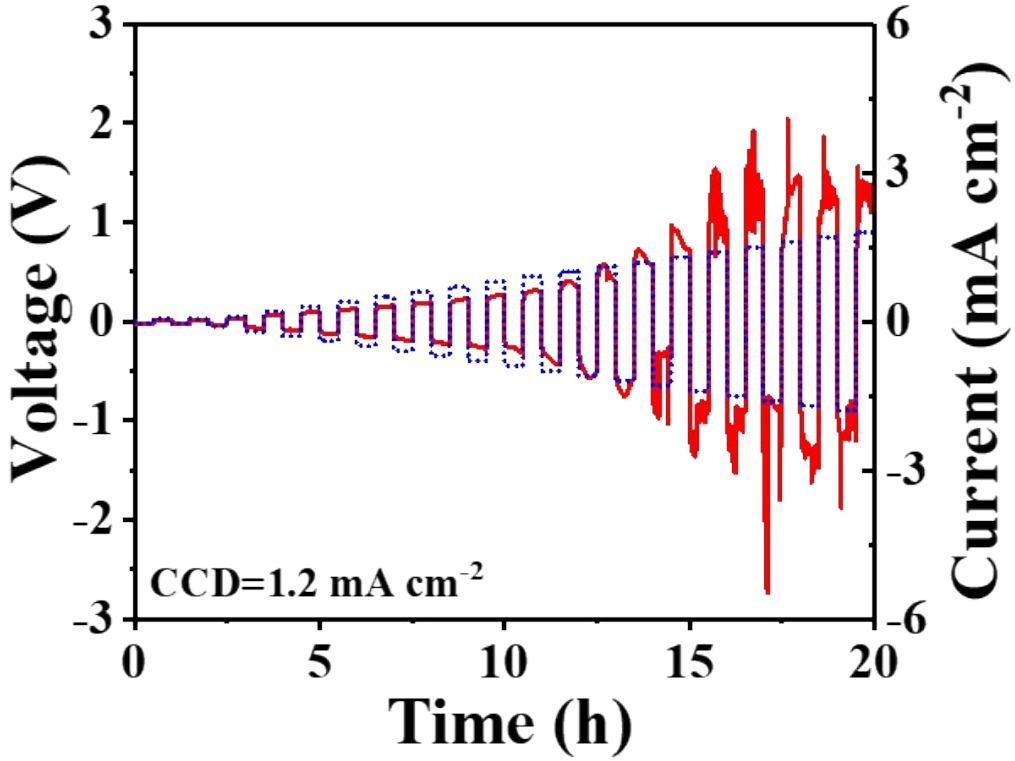

Fig. S10 The CCD test of PCL-DDCA electrolyte.

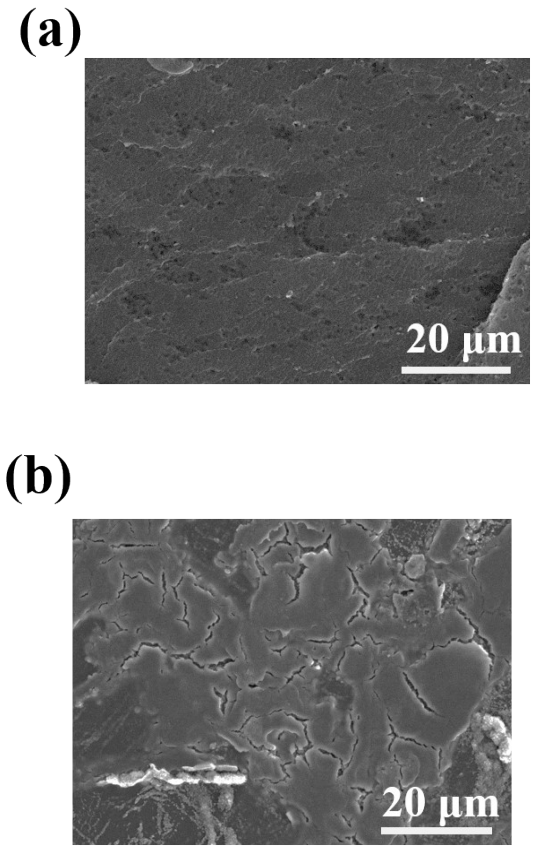

Fig. S11 SEM images of Li metal surface in symmetric cells with (a) PCL-DDCA-PC, (b) PCL-DDCA after cycling.

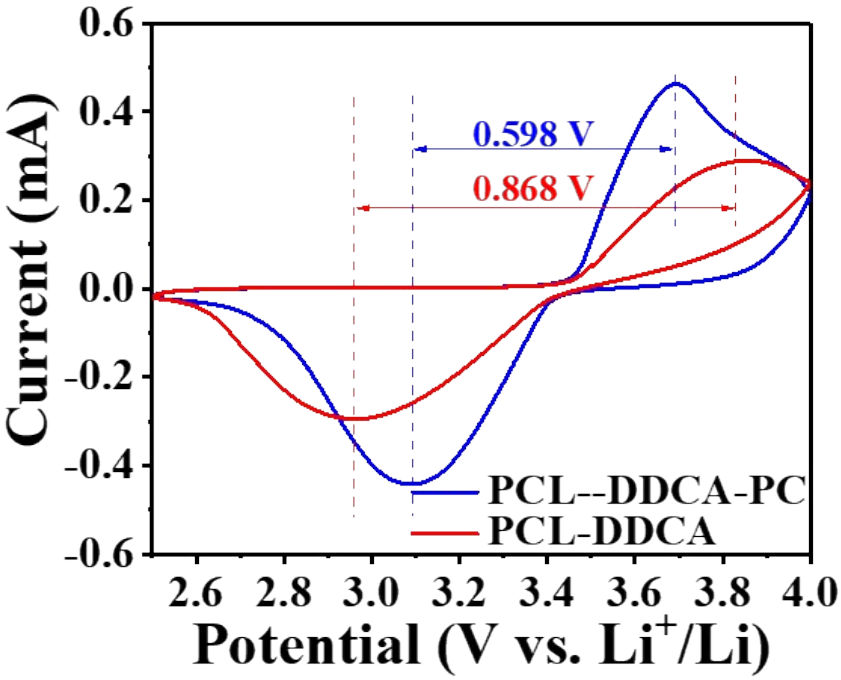

Fig. S12 The CV curves of different electrolyte.

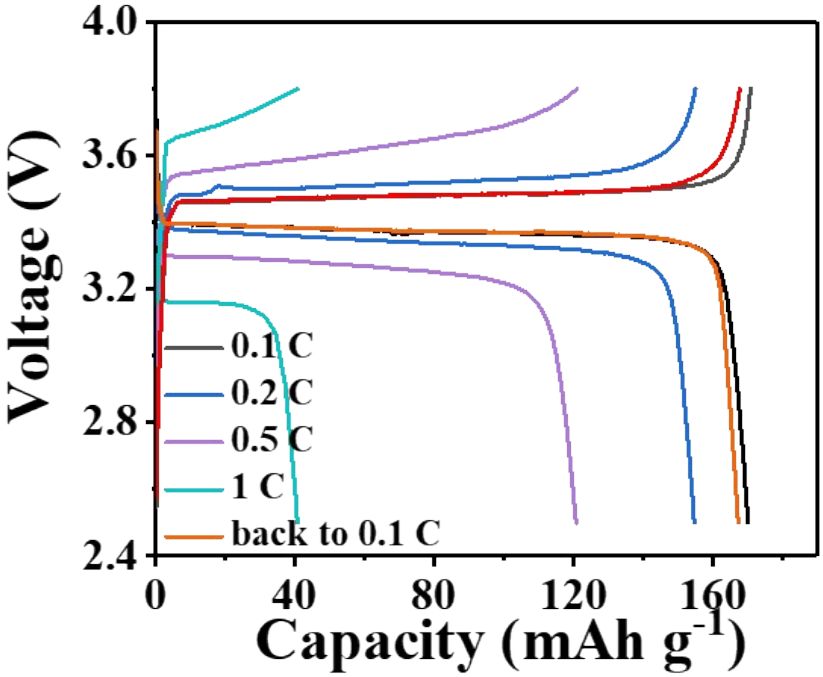

Fig. S13 Charge/discharge profiles of $LiFePO_4$//Li full cells with PCL-DDCA electrolyte at various current densities.

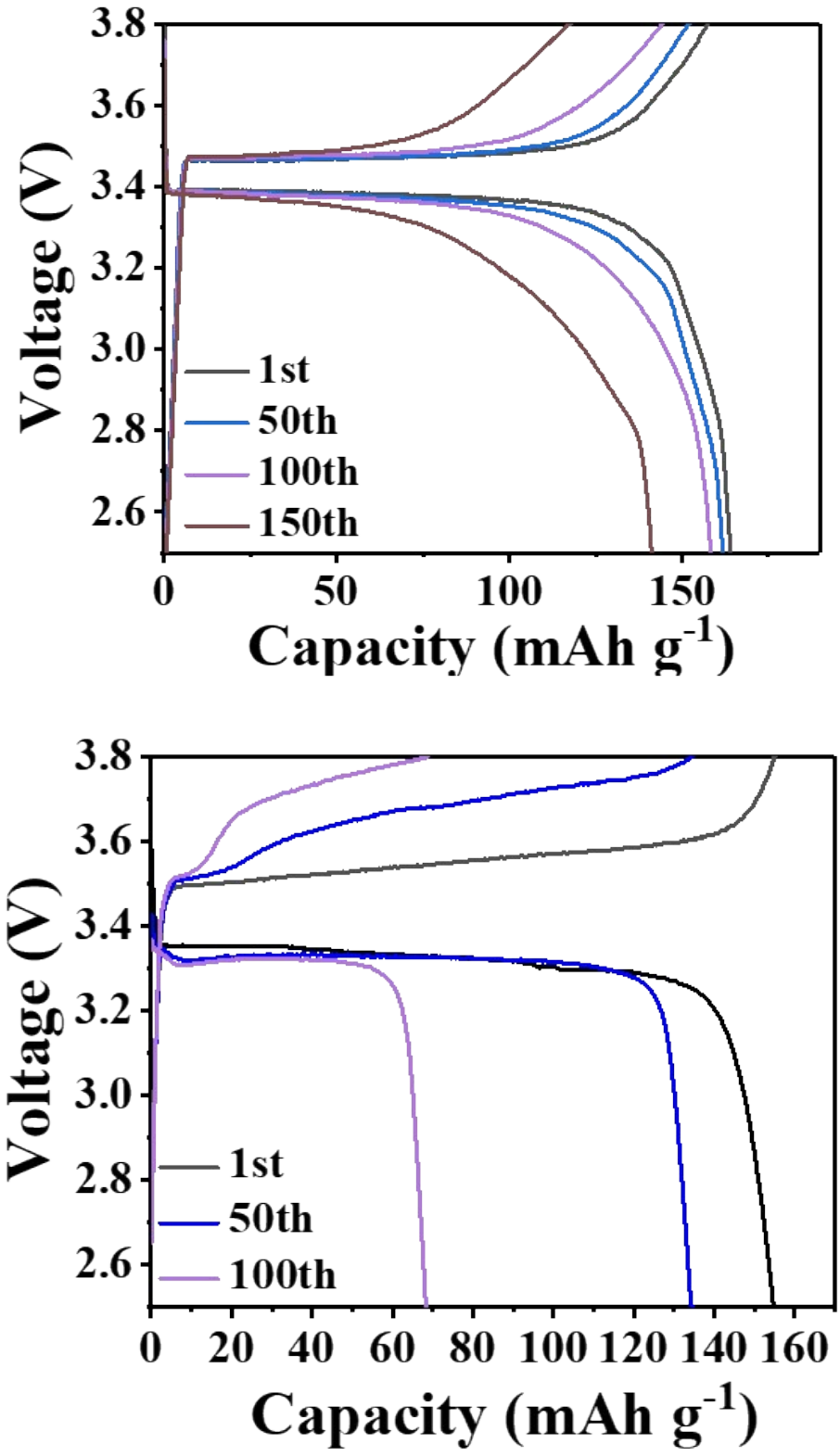

Fig. S14 Galvanostatic charge/discharge cycling curves of $LiFePO_4$//Li full cells with PCL-DDCA-PC electrolyte (top) and PCL-DDCA (bottom) at 0.2 C.

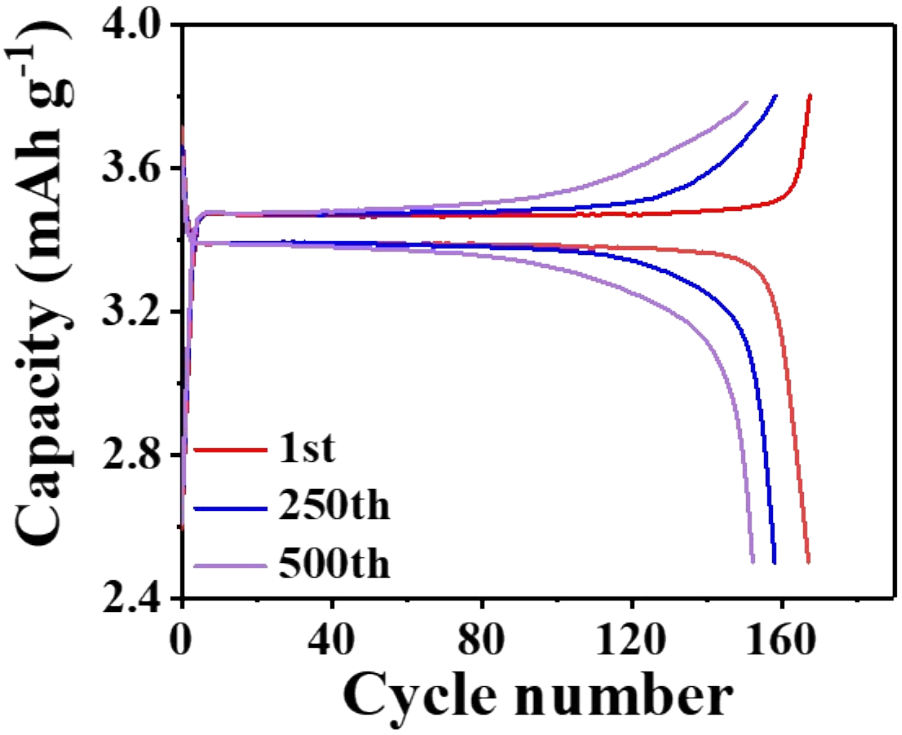

Fig. S15 Galvanostatic charge/discharge cycling curves of $LiFePO_4$//|Li full cells with PCL-DDCA-PC electrolyte at 0.5 C.

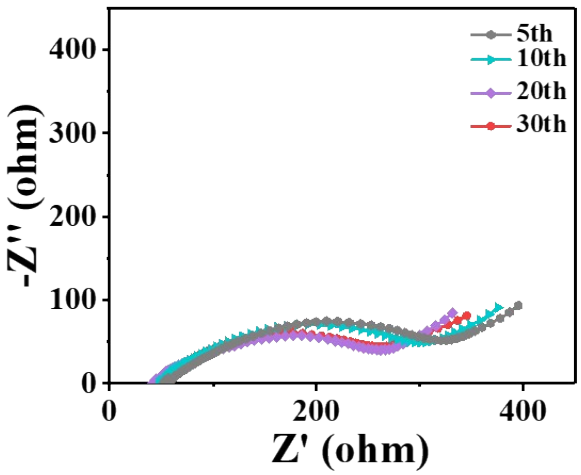

Fig. S16. EIS spectra of LFP||PCL-DDCA-PC||Li of different cycles at 0.5 C.

Fig. S17 Photograph of Li/PCL-DDCA-PC electrolyte/$LiFePO_4$ pouch-type cell lighting up the red LED panel.

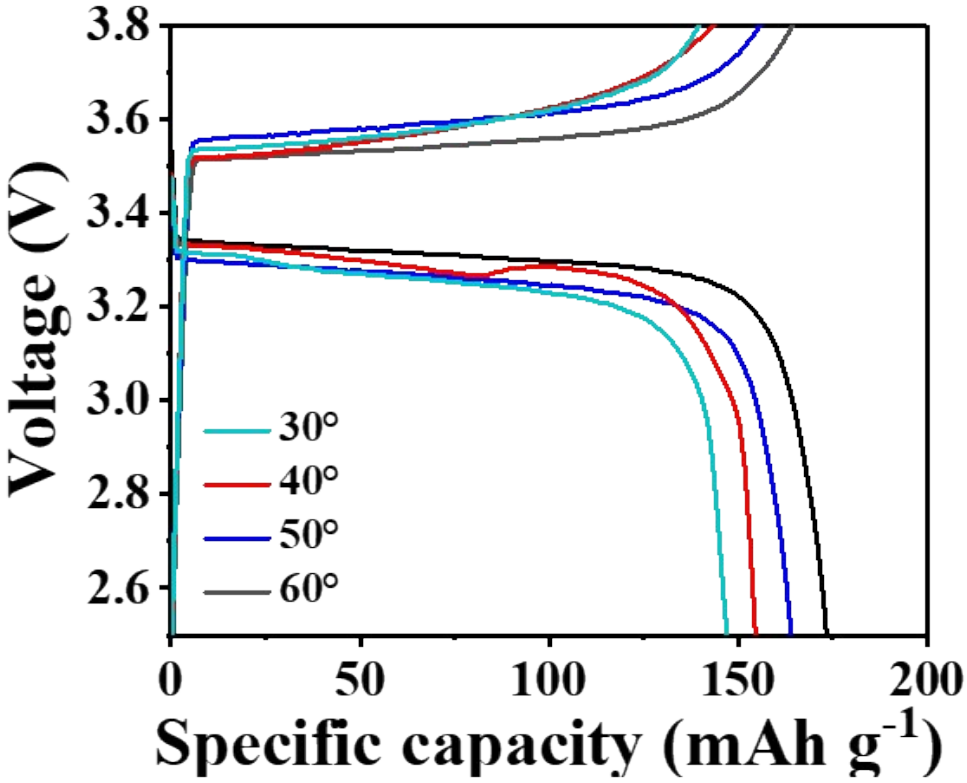

Fig. S18 Temperature-dependent charge-discharge voltage profiles of Li/PCL-DDCA-PC electrolyte/$LiFePO_4$.

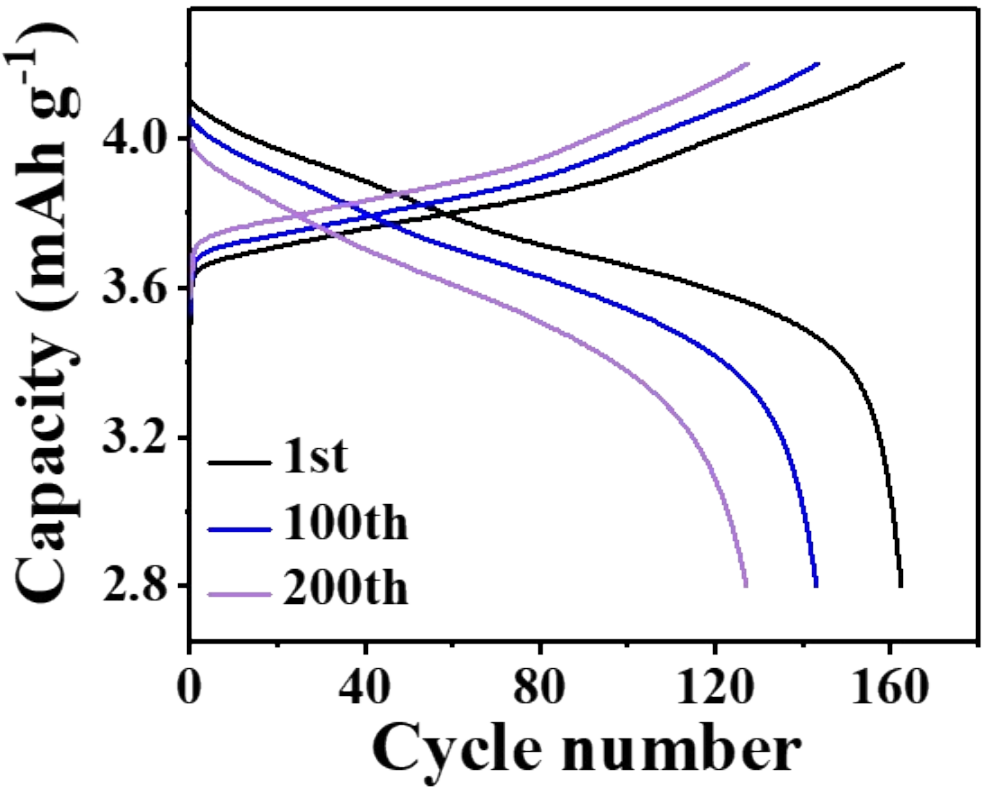

Fig. S19 Charge-discharge voltage profiles of Li/PCL-DDCA-PC electrolyte/NCM811 at 0.5 C.

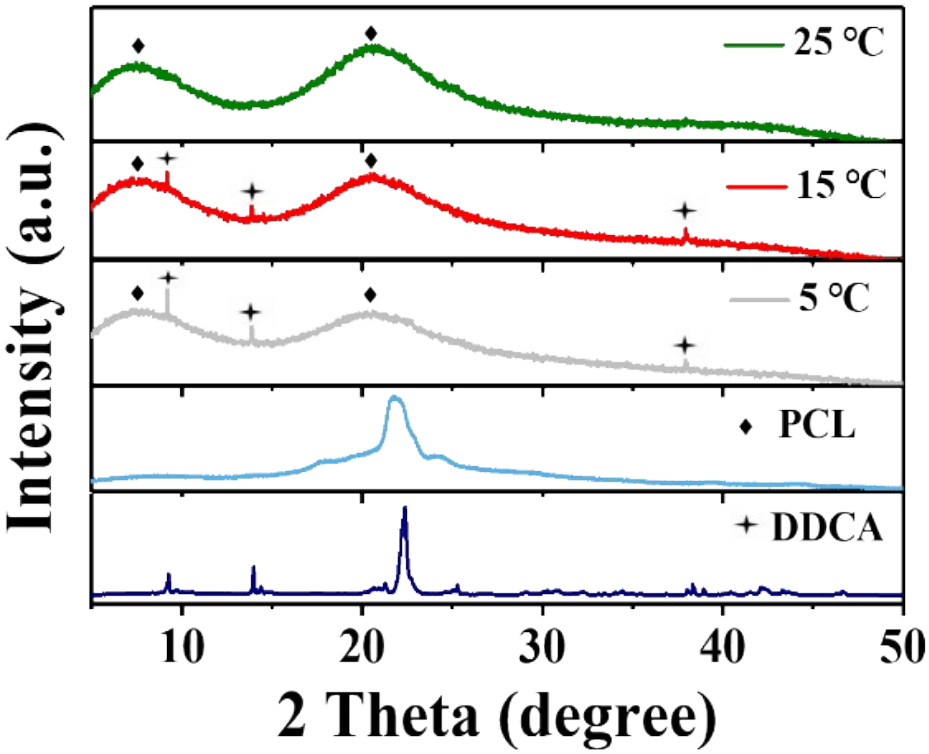

Fig. S20 X-ray diffraction (XRD) patterns of the components and PCL-DDCA-PC electrolyte at variable temperatures.

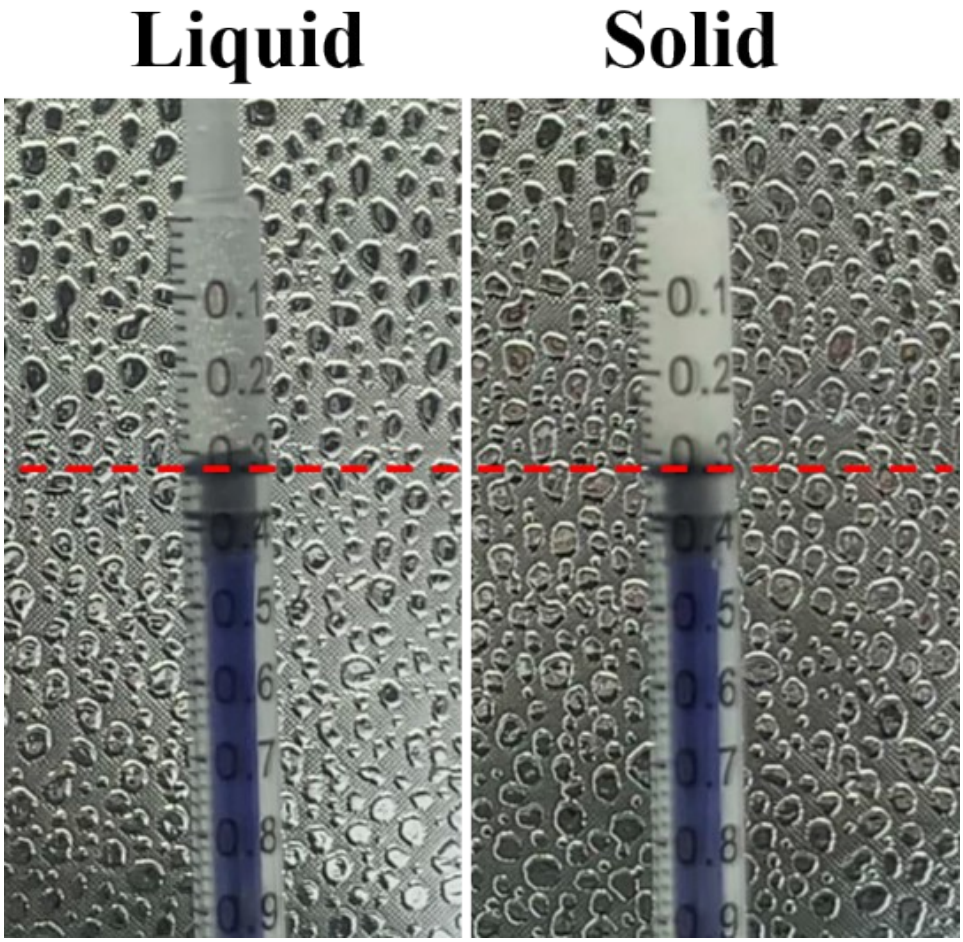

Fig. S21 The comparison of volume between liquid-state PCL-DDCA-PC electrolyte and solid-state PCL-DDCA-PC electrolyte.

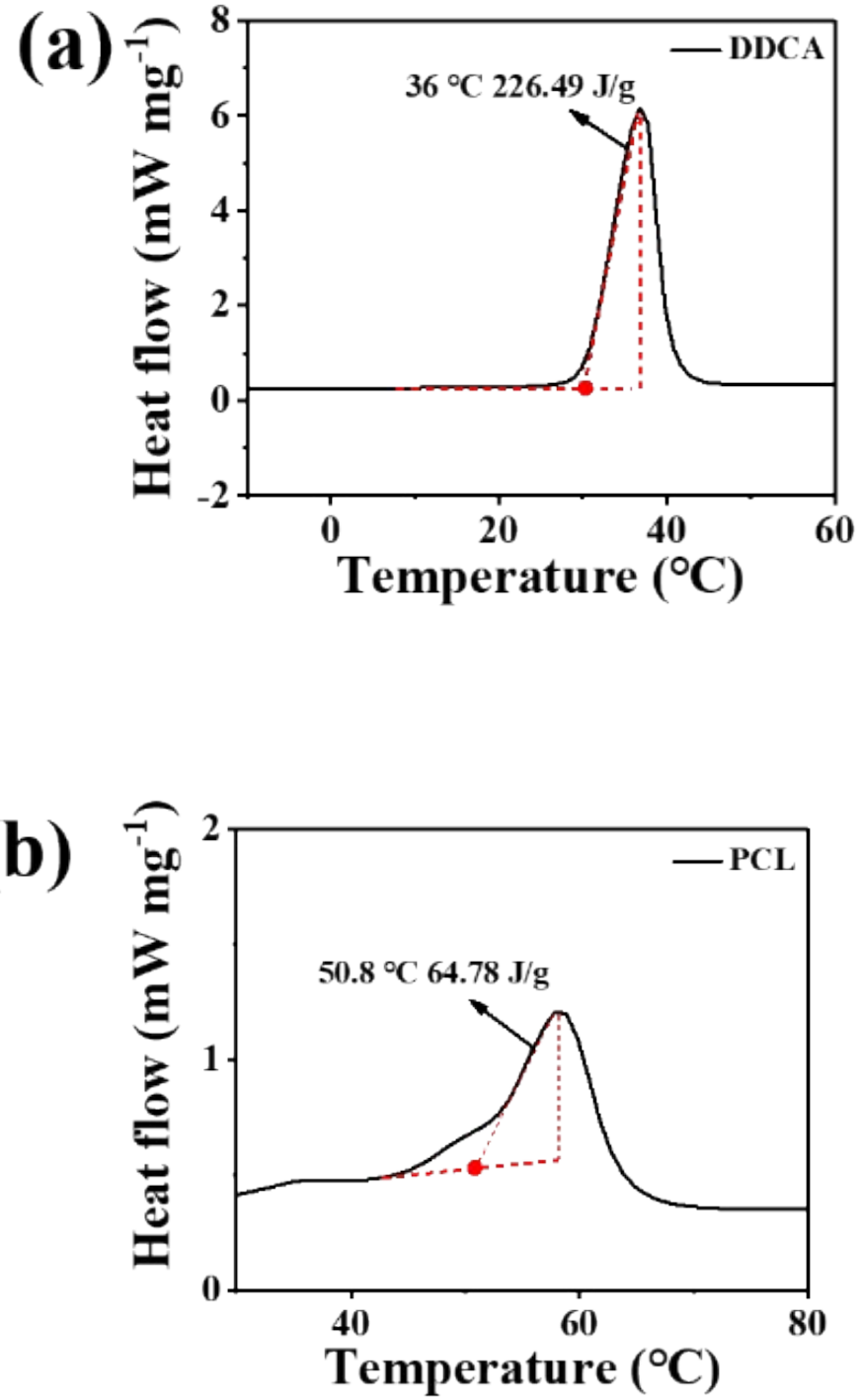

Fig. S22 DSC curves of (a) DDCA and (b) PCL.

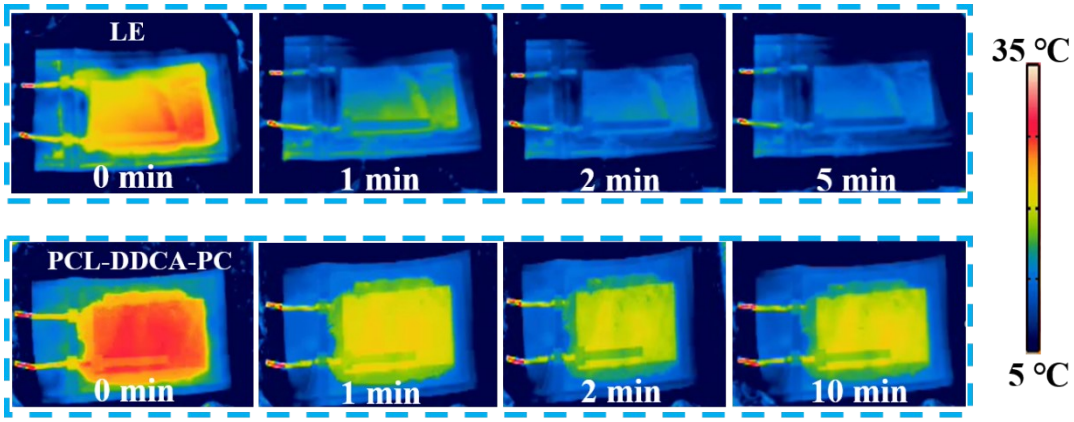

Fig. S23 Thermal imaging images of pouch cells with the construction of (a) Li/ PCL-DDCA-PC electrolyte/LFP and (b) Li/ LE/LFP frozen at 5 °C.

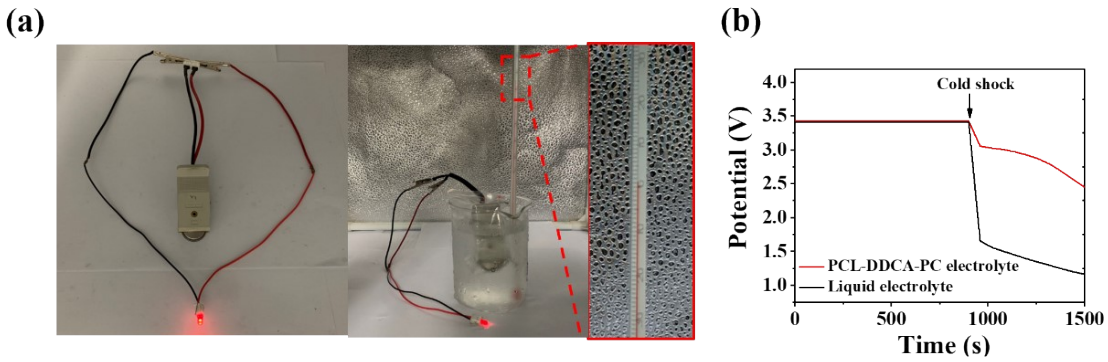

Fig. S24 (a) Optical image of a led bulb powered by Li||LFP cells with the PCL-DDCA-PC electrolyte at 0 °C. (b) Variation in the open-circuit potential of battery assembled with PCL-DDCA-PC electrolyte or liquid electrolyte upon cold shock (0 °C).

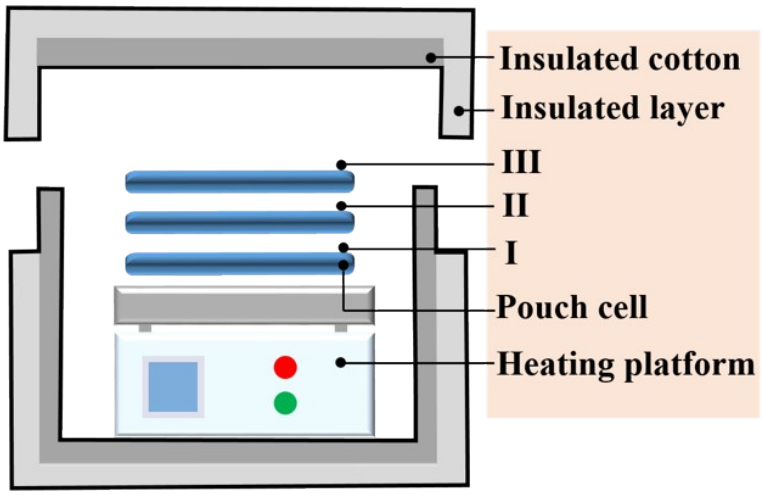

Fig. S25 Schematic of the insulated box.

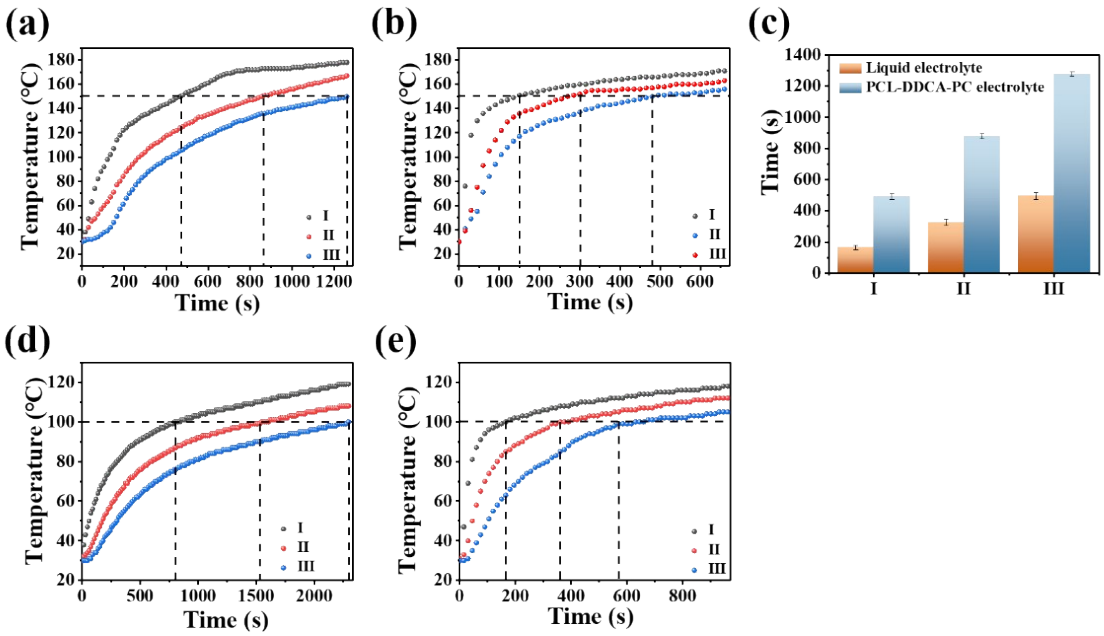

Fig. S26 When the heating platform is set to 150 ℃, temperature of different positions versus time in (a) PCL-DDCA-PC electrolyte system and (b) liquid electrolyte system. (c) The comparison of time required to reach the 150 ℃ at different positions in PCL-DDCA-PC electrolyte and liquid electrolyte. When the heating platform is set to 100 ℃, temperature of different positions versus time in (d) PCL-DDCA-PC electrolyte system and (e) liquid electrolyte system.

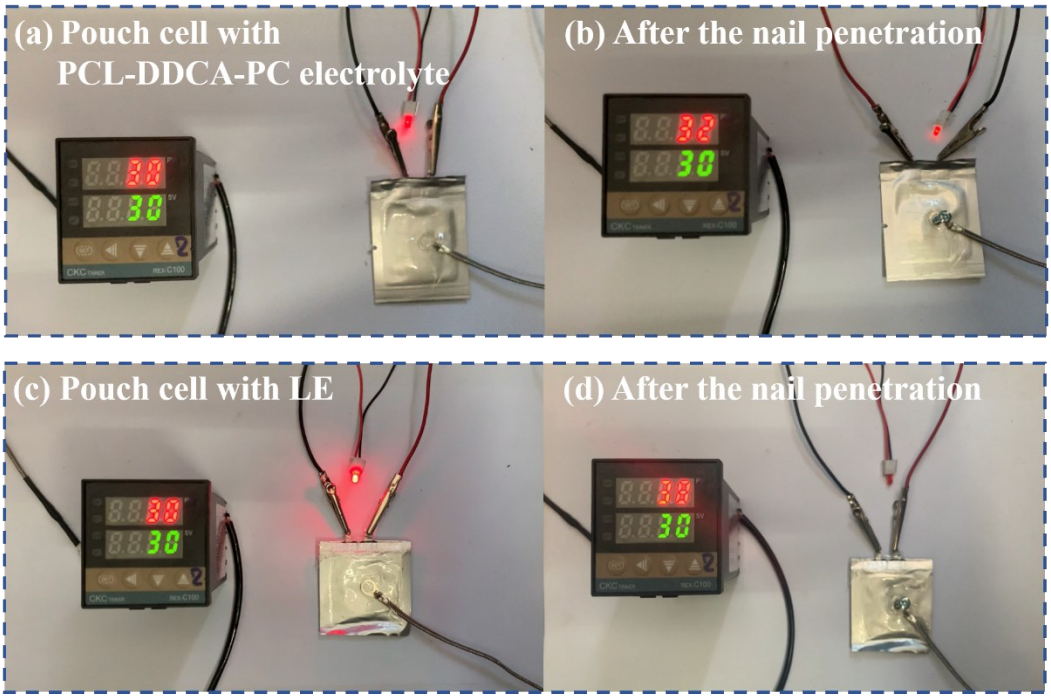

Fig. S27 Pictures of Li||LFP pouch cell using (a-b) PCL-DDCA-PC electrolyte and (c-d) liquid electrolyte before and after the nail penetration.

Table S1. Comparison between PCL-DDCA-PC electrolyte and other PCL or PEO based electrolytes.

Electrolyte configuration	**Ionic conductivity (S cm^{-1})**	**Electrochemical Window (vs Li$^+$/Li)**	**Full cell performance(mAh g^{-1})**	Reference
PCL-DDCA-PC-electrolyte (this work)	3.38×10^{-4}	**4.6V**	**151.6 at 0.5C**	This work
PEG-PCL	1.45×10^{-4}	4.54	128.1 at 0.3C (60 °C)	[1]
PCL-LiTFSI-Cyclodextrin	1.0×10^{-4}	4.6V	120 at 1 C	[2]
PCL−$LiClO_4$−LATP	3.64×10^{-5} (55℃)	5V	136.6 at 0.3C	[3]
PCL-LiTFSI	2.5 × 10-5	Not mentioned	140 at 0.1C	[4]
PCL-LiTFSI-LAGP	1.7×10^{-4}	5V	157 at 0.1C	[5]
PCL-LiTFSI-LATP	Not mentioned	4.2V	137.8 at 0.5C	[6]
PCL/PS copolymer-LiFSI	1.35×10^{-5} （80℃）	4.6V	133 at 1C	[7]
PEO-LiTFSI-LLZO	1.2×10^{-4}	5V	128 at 0.5C (60℃)	[8]

1. Y. Li, K. Zhu, H. Bu, Z. Fu, A.-L. Kjøniksen, B. Nyström and S. Ding, *Macromolecules*, 2023, **56**, 7921-7930.
2. L. Imholt, T. S. Dörr, P. Zhang, L. Ibing, I. Cekic-Laskovic, M. Winter and G. Brunklaus, *J. Power Sources*, 2019, **409**, 148-158.
3. Y. Li, M. Liu, S. Duan, Z. Liu, S. Hou, X. Tian, G. Cao and H. Jin, *ACS Appl. Energy Mater.*, 2021, **4**, 2318-2326.
4. Y. Seo, Y.-C. Jung, M.-S. Park and D.-W. Kim, *J. Membr. Sci.*, 2020, **603**, 117995.
5. B. Zhang, Y. Liu, J. Liu, L. Sun, L. Cong, F. Fu, A. Mauger, C. M. Julien, H. Xie and X. Pan, *Journal of Energy Chemistry*, 2021, **52**, 318-325.
6. Y. Li, F. Wang, B. Huang, C. Huang, D. Pei, Z. Liu, S. Yuan, S. Hou, G. Cao and H. Jin, *Electrochim. Acta*, 2022, **424**, 140624.
7. W. Ye, M. Zaheer, L. Li, J. Wang, H. Xu, C. Wang and Y. Deng, *J. Electrochem. Soc.*, 2020, **167**, 110532.
8. Z. Li, W.-X. Sha and X. Guo, *ACS Appl. Mater. Interfaces*, 2019, **11**, 26920-26927.